

Hopping conductivity in CaCu_2O_3 single crystals

This article has been downloaded from IOPscience. Please scroll down to see the full text article.

2006 J. Phys.: Condens. Matter 18 8541

(<http://iopscience.iop.org/0953-8984/18/37/012>)

View [the table of contents for this issue](#), or go to the [journal homepage](#) for more

Download details:

IP Address: 129.252.86.83

The article was downloaded on 28/05/2010 at 13:44

Please note that [terms and conditions apply](#).

Hopping conductivity in CaCu_2O_3 single crystals

K G Lisunov¹, E Arushanov¹, B Raquet², J M Broto², F C Chou^{3,5},
N Wizen⁴ and G Behr⁴

¹ Institute of Applied Physics, Academy of Sciences of Moldova, Academiei Street 5,
MD-2028 Kishinev, Moldova

² Laboratoire National des Champs Magnétiques Pulsés, 31432 Toulouse Cedex 04, France

³ Center for Materials Science and Engineering, Massachusetts Institute of Technology,
Cambridge, MA 02139, USA

⁴ Leibniz Institute for Solid State and Materials Research, IFW Dresden, D-01171 Dresden,
Germany

Received 8 June 2006, in final form 10 July 2006

Published 1 September 2006

Online at stacks.iop.org/JPhysCM/18/8541

Abstract

The resistivity, ρ , of the spin-ladder compound CaCu_2O_3 is investigated between $T \sim 130$ –450 K. The $\rho(T)$ data measured for $\mathbf{j} \parallel \mathbf{b}$ (along the Cu–O–Cu leg) and $\mathbf{j} \parallel \mathbf{a}$ (along the Cu–O–Cu rungs), $\rho_a(T) > \rho_b(T)$, exhibit an activated dependence, similar in both directions and characterized by a nearest-neighbour hopping followed by a variable-range hopping (VRH) regime when T is decreased. A detailed analysis of $\rho(T)$ demonstrates that conventional d -dimensional models of the hopping conductivity, based on the electron localization in disordered systems, cannot interpret the experimental data at any $d = 1, 2$ or 3 , leading to the mismatch of the characteristic energies and/or unphysical values of the characteristic length scales. The observed VRH conductivity law on the low-temperature interval, $\ln \rho \sim T^{-3/4}$, contradicts the models above, too. Instead, it is found that this law can be substantiated and the correct matching of the energy and length scales can be found within a model of Fogler *et al* (2004 *Phys. Rev. B* **69** 035413) by treating CaCu_2O_3 as a three-dimensional array of quasi-one-dimensional electron crystals.

(Some figures in this article are in colour only in the electronic version)

1. Introduction

In recent years much attention has been paid to the so-called spin-ladder systems owing to the prediction of the presence of spin-gap and possible appearance of the ‘d-wave’ superconductivity in the hole-doped even-leg systems [1–3]. The ladder systems are considerably easier to study theoretically than two-dimensional models because they are

⁵ Present address: Centre of Condensed Matter Sciences, National Taiwan University, Taipei 106, Taiwan.

basically quasi-one-dimensional and they can provide a playground for studies of high-critical-temperature superconductors [3].

CaCu_2O_3 , belonging to the ladder family, has not yet been well studied. CaCu_2O_3 has a geometry very similar to the well-known spin-ladder material SrCu_2O_3 . However, SrCu_2O_3 has a planar Cu–O–Cu structure (180°). In contrast to this, the compound CaCu_2O_3 consists of an array of linear Cu–O–Cu legs coupled through buckled Cu–O–Cu rungs (123°) to form ladders [4]. Recently, high-quality bulk CaCu_2O_3 single crystals [4, 5] as well as $[\text{CaCu}_2\text{O}_3]_4$ [6] thin films have been prepared and characterized.

CaCu_2O_3 shows an unusual non-planar hole distribution at variance with conventional ladder compounds [7]. In contrast to the undoped two-leg ladder compounds, undoped CaCu_2O_3 is an antiferromagnet [4], like other two-dimensional parent compounds. Therefore, this compound can be considered as an anisotropic layer compound and a candidate for high-temperature superconductivity at hole doping away from the antiferromagnetic insulating state investigated so far [7, 8].

Here, we report on the conductivity of the two-leg CaCu_2O_3 single crystals. The investigations are expected to yield important information about the mechanisms of charge transfer, the energy spectrum, and the properties of charge carriers in this material.

2. Results and discussion

CaCu_2O_3 has an orthorhombic lattice, space group $Pmnm$, with lattice parameters $a = 9.949 \text{ \AA}$, $b = 4.078 \text{ \AA}$ and $c = 3.460 \text{ \AA}$ at $T = 10 \text{ K}$. Single crystals of CaCu_2O_3 were grown using the travelling solvent floating zone (TSFZ) method with a CuO-rich solvent. The growth was carried out in a four-lamp optical FZ furnace built by Crystal Systems Inc., under flowing O_2 doped with about 8% Ar. The growth direction in the obtained crystals is approximately parallel to the copper oxide chain \mathbf{b} [010] direction [4]. The electron probe microanalysis data taken at ten points of the crystal surface of size $2 \times 2 \text{ mm}^2$ reveal the following composition of the elements. Ca: 0.854 (0.023), Cu: 2.039 (0.056) and O: 3.005 (0.082). We note that an appreciable excess of Cu and a respective deficiency of Ca are quite typical for this material [5].

The resistivity, ρ , was measured in zero magnetic field and in pulsed fields up to $B = 45 \text{ T}$, using silver paint on evaporated gold contacts and the geometry of $\mathbf{j} \parallel \mathbf{b}$ and $\mathbf{j} \parallel \mathbf{a}$ [100] (or, more strictly, with \mathbf{j} having a small angle with the \mathbf{a} direction of the sample) in investigations of $\rho(T)$ at $B = 0$, the cases marked below as # 2b and # 2a, respectively, whereas the magnetoresistance (MR) was measured at $\mathbf{j} \parallel \mathbf{b}$, $\mathbf{B} \parallel \mathbf{c}$ [001] and $\mathbf{j} \parallel \mathbf{B} \parallel \mathbf{b}$ at constant $T = 237 \text{ K}$. Special care was taken in the electronic conductivity experiments using a home-made high impedance voltage amplifier. The transport measurements with $\mathbf{j} \parallel \mathbf{b}$ were both performed with two and four probes, revealing identical temperature dependences of the resistance.

As can be seen from figure 1, $\rho(T)$ at $B = 0$ has a similar strongly activated character in both cases of # 2a and # 2b with $\rho_a(T)$ (# 2a) exceeding measurably $\rho_b(T)$ (# 2b). The MR $\Delta\rho/\rho = [\rho(B) - \rho(0)]/\rho(0)$ (not shown) does not exhibit a systematic variation with the magnetic field up to $B = 45 \text{ T}$ within an error of $\Delta\rho/\rho \sim 1.5\%$, both with increasing and decreasing B .

The $\rho(T)$ dependences in figure 1 suggest electron localization and hopping charge transfer. A nearest-neighbour hopping (NNH) conductivity with the Arrhenius law,

$$\rho(T) = \rho_{0n} \exp[E_a/(kT)], \quad (1)$$

where E_a is the activation energy and ρ_{0n} is the prefactor (generally, ρ_{0n} has a weak power-law dependence on T , which can be neglected comparing with a much stronger exponential one as

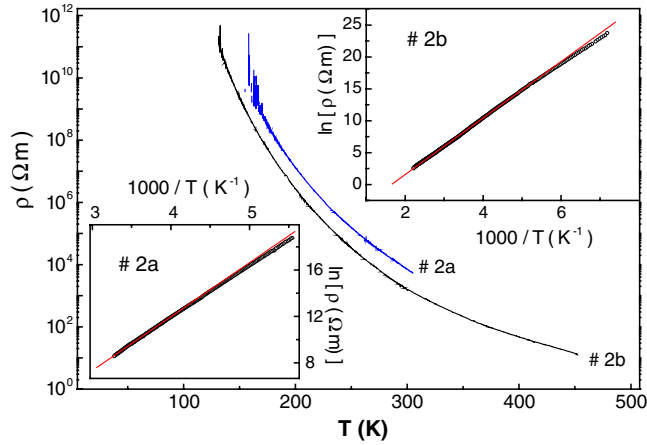


Figure 1. Temperature dependence of the resistivity for #2b and #2a. Insets: $\ln \rho$ versus $1/T$ for #2a and #2b.

far as $\rho(T)$ varies by several orders of the magnitude), follows from the plots of $\ln \rho$ versus $1/T$ in the insets of figure 1 down to the temperatures $T_n \approx 189$ K and 236 K for #2b and #2a, respectively. The linear fit of the plots in the insets of figure 1 with equation (1) yields $\rho_{0n} = 6.82 \times 10^{-4} \Omega \text{ m}$, $E_a = 0.38$ eV for #2b and $\rho_{0n} = 1.32 \times 10^{-3} \Omega \text{ m}$, $E_a = 0.40$ eV for #2a. It is worth mentioning a similar value of $E_a \approx 0.28$ eV obtained in another copper–oxygen spin chain/ladder compound, $\text{La}_3\text{Sr}_3\text{Ca}_8\text{Cu}_{24}\text{O}_{41}$ [9]. Below T_n the resistivity deviates from equation (1), which is attributable to the variable-range hopping (VRH) conductivity satisfying a general law [10, 11]

$$\rho(T) = \rho_{0v} \exp[(T_0/T)^p], \quad (2)$$

where ρ_{0v} is the prefactor, T_0 is the characteristic temperature and the values of the exponent p are specified below. Usually the VRH conductivity is analysed within the Mott ($p = 1/4$) [10] or the Shklovskii–Efros (SE, $p = 1/2$) [11] concepts, depending on the importance of the Coulomb interaction between the localized electrons. The Mott VRH conductivity sets in with lowering T for non-interacting electrons in disordered materials, when thermal excitations of the electrons are insufficient for jumping to the nearest sites with large energy difference and hopping to the more distant sites with a smaller energy differences is favourable [10]. The long-range Coulomb interaction leads to a soft Coulomb parabolic gap, Δ , in the density of states (DOS) of the localized electrons, ($E_F - \Delta$, $E_F + \Delta$), around the Fermi energy E_F , leading to the SE VRH conductivity law [11].

As can be seen from figure 2, within an interval below the temperature $T_M \approx 152$ K (#2b) and 189 K (#2a) the plots of $\ln \rho$ versus $T^{-1/4}$ can be fitted approximately with a linear law, yielding the values of $\rho_{0v} = 2.39 \times 10^{-40} \Omega \text{ m}$, $4.14 \times 10^{-35} \Omega \text{ m}$ and $T_0 = 2.43 \times 10^{10}$ K, 1.66×10^{10} K for #2b and #2a, respectively. Besides the unphysically low values of ρ_{0v} , those of T_M and T_0 are also contradictory. Indeed, within the Mott concept we have $E_a \approx \Delta E$, the width of the electron band due to disorder. On the other hand, the onset of the Mott VRH regime satisfies the condition of $\Delta \varepsilon_{\text{max}} \equiv k(T_0 T_M^3)^{1/4} < \Delta E$, where $\Delta \varepsilon_{\text{max}}$ is the maximum value of the Mott’s optimum stripe or the hopping energy [11]. However, with the values above we find $\Delta \varepsilon_{\text{max}} \approx 1.5\text{--}1.6$ eV to be ~ 4 times wider than ΔE , which completely disagrees with the assumption of the Mott VRH regime.

As follows from figure 2, the fits of the low-temperature data of $\rho(T)$ to the SE VRH law with $p = 1/2$ can be done within a wider intervals, below the temperature $T_{\text{SE}} \approx 170$ K (#2b)

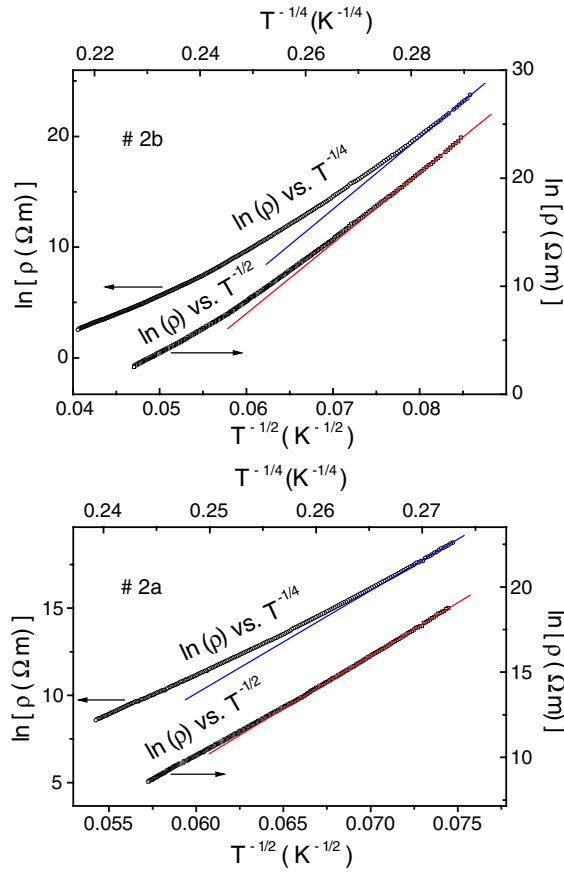


Figure 2. The plots of $\ln \rho$ versus $T^{-1/4}$ and $\ln \rho$ versus $T^{-1/2}$ for # 2b (upper panel) and # 2a (lower panel).

and 215 K (# 2a), giving $\rho_{0v} = 1.71 \times 10^{-14} \Omega \text{ m}$, $1.08 \times 10^{-12} \Omega \text{ m}$ and $T_0 = 4.28 \times 10^5 \text{ K}$, $3.87 \times 10^5 \text{ K}$ for # 2b and # 2a, respectively. However, the width of the Coulomb gap, $\Delta \approx k(T_0 T_{SE})^{1/2}/2 = 0.37 \text{ eV}$ (# 2b) and 0.39 eV (# 2a), evaluated with the values above, excludes any observations of the NNH conductivity because we have $\Delta \approx E_a \approx \Delta E$, i.e. all the states of the band of the localized electrons should lie inside the Coulomb gap, contradicting the linearity of the plots in figure 1 (insets) on the high-temperature interval. In addition, with the expression $T_0 = \beta e^2 / (k\kappa\xi)$ which takes place in the SE VRH regime, where κ is the dielectric constant, ξ is the localization radius scaling an exponential decay of the wavefunctions of the localized electrons, $\psi(r) \sim \exp(-r/\xi)$, and $\beta = 2.8$ is a constant, we find the values of $\kappa\xi \approx 1.1\text{--}1.2 \text{ \AA}$, which for reasonable values of $\kappa > 10$ lead to unphysical values of $\xi < 0.1 \text{ \AA}$.

The analysis above suggested a three-dimensional (3D) VRH regime. However, it can be shown that similar contradictions persist if the two-dimensional (2D) hopping is assumed. For example, for a 2D Mott VRH conductivity we have $p = 1/3$ in equation (2) [11], and the corresponding fit of the experimental $\rho(T)$ data (not shown) gives for # 2b $T_0 = 7.78 \times 10^7 \text{ K}$, $T_M \approx 165 \text{ K}$ and $\Delta\varepsilon_{\text{max}} = k(T_0 T_M^2)^{1/3} \approx 1.1 \text{ eV}$. Also the absence MR in the domain of the NNH conductivity ($T = 237 \text{ K}$) is contradictory. Indeed, under the condition of $\lambda/\xi \gg 1$ (λ is the magnetic length) which is fulfilled for ξ between 1 and 40 \AA , the MR can be written as

$\Delta\rho/\rho = \exp(\gamma B^2) - 1 \approx \gamma B^2$, where $\gamma = 0.036\xi e^2/(N_s\hbar^2)$ and N_s is the concentration of sites [11]. Then from the relation $\Delta\rho/\rho < 1.5\%$ above we find $N_s > 1 \times 10^{24} \text{ cm}^{-3}$ already for $\xi = 1 \text{ \AA}$, which exceeds the total concentration of atoms in the compound.

The values of the electron transfer (hopping) integrals, t , evaluated in [12] for CaCu₂O₃ satisfy the approximate relations $t_{\text{leg}}:t_{\text{rung}}:t_{\text{inter}} \approx 5:2:1$, where t_{leg} , t_{rung} and t_{inter} are the values of t in the directions along the leg **b**, the rungs **a** and along an intermediate direction in the a - b plane of the CaCu₂O₃ structure, respectively. This may provide a possibility of a good quasi-one-dimensional (1D) hopping regime for # 2b and a less good one for # 2a as well. On the other hand, the relation $t_{\text{leg}} > t_{\text{rung}}$ is in line with the corresponding relation $\rho_a > \rho_b$ evident from figure 1. The arguments above permit us to examine 1D hopping models to interpret the conductivity of our material.

The first model to be discussed (Yu *et al* [13]) deals with non-interacting electrons in isolated disordered 1D structures like macromolecules. It suggests the NNH regime satisfying equation (1) at $T > T_c$ and the VRH conductivity given by equation (2) with $p = 1/2$ at $T < T_c$, where $E_a = \Delta E$ (the width of the 1D electron band due to disorder),

$$T_0 = 8\Delta ER\alpha/k_B, \quad T_c = \Delta E/(2R\alpha k_B), \quad (3)$$

$\alpha \equiv \xi^{-1}$ and R is the distance between the sites. It can be seen that the values of E_a and T_0 found above from figures 1 and 2 (with the plots of $\ln \rho$ versus $T^{-1/2}$), respectively, can be utilized directly, whereas for T_c we can take the average values between T_n and T_{SE} , $T_c = 179 \pm 10 \text{ K}$ and $226 \pm 10 \text{ K}$ for # 2b and # 2a, respectively. From the product of equations (3) we find $\Delta E = k(T_0 T_c)^{1/2}/2 \approx 0.38 \text{ eV}$ (# 2b) and 0.40 eV (# 2a), which coincide with the corresponding values of E_a in agreement with predictions of the model [13]. From the two equations (3) we find for # 2a the values of $\alpha R = 10.4$ and 9.8 , respectively, and for # 2b $\alpha R = 12.1$ and 12.3 , respectively. These relations are good in the sense that they match well when evaluated with different experimentally found parameters, T_0 and T_c . On the other hand, assuming that hopping is over the Cu sites (e.g. similar to La₃Sr₃Ca₈Cu₂₄O₄₁ [9]) and taking $R_{\text{leg}} = 4.1 \text{ \AA}$ and $R_{\text{rung}} = 3.3 \text{ \AA}$, where R_{leg} and R_{rung} are the values of R along the leg and along the rungs of the ladder CaCu₂O₃ structure, respectively [12], we find again the unphysically small value of $\xi \approx 0.3 \text{ \AA}$. Another weak point of this model will be demonstrated later.

Serota *et al* [14] proposed a percolation model of 1D VRH conductivity which takes into account a finite length, L , of a 1D chain. No electron correlations have been suggested, as well. The same equation (2) with $p = 1/2$ has been established for $T < T_c$, whereas equations (3) are changed to

$$T_0 = 2x\Delta ER\alpha/k_B, \quad T_c = \Delta E/(2x\alpha Rk_B), \quad (3')$$

respectively, where all the parameters have the same meanings as in the previous 1D model [13] and $x = \ln(2\alpha L)$. For a macroscopic sample we have $L \approx 1\text{--}5 \text{ mm}$, so that for the reasonable values of $\xi = 1\text{--}1.5 \text{ \AA}$ (not exceeding $R/2$) we find $L = 17 \pm 1$. Then with the first and the second of equations (3') and the values of R_{leg} and R_{rung} above we find $\xi = 1.4$ and 5.6 \AA (# 2b), $\xi = 1.7$ and 6.8 \AA (# 2a), respectively. Also from the product of equations (3') we obtain $\Delta E = k(T_0 T_c)^{1/2} = 0.75 \text{ eV}$ (# 2b) and 0.80 eV (# 2a). The values of $\xi = \alpha^{-1}$ found with the first of equations (3') are reasonable. However, those found with the second of equation (3') are ~ 5 times higher and the values of ΔE are ~ 2 times higher than E_a , making this model inapplicable to the case of CaCu₂O₃, too.

A poor applicability of the 1D hopping models above to our $\rho(T)$ data is confirmed by a more thorough analysis of the resistivity, exhibiting that a low-temperature VRH conductivity law $\ln \rho \sim T^{-1/2}$, suggested in both models [13, 14], does not exist at all. Indeed, the value of the exponent p in equation (2) can be found independently by analysing the local

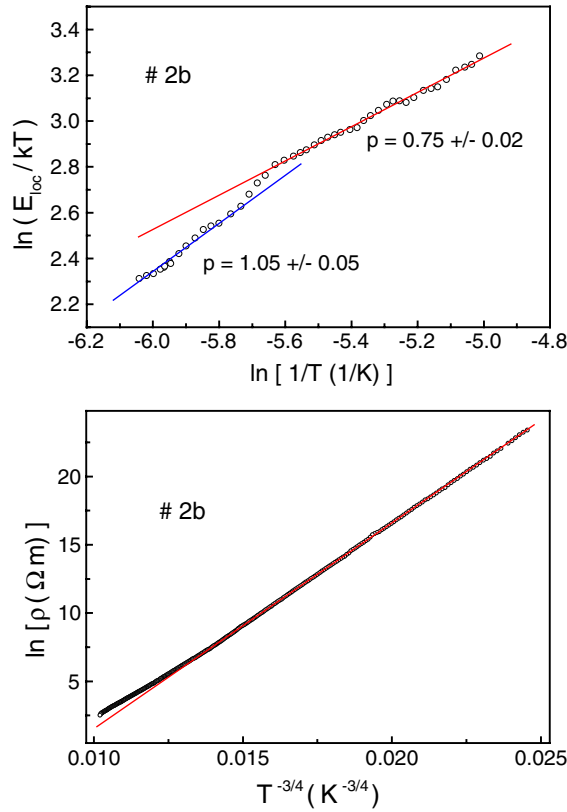


Figure 3. (a) Temperature dependence of the local activation energy (upper panel) and the plot of $\ln \rho$ versus $T^{-3/4}$ for # 2b (lower panel).

activation energy, $E_{\text{loc}} \equiv d \ln \rho / d(kT)^{-1}$ [11]. Neglecting a weak temperature dependence of the prefactor we find, with equation (2), $\ln[E_{\text{loc}}/(kT)] = \ln p + p \ln T_0 + p \ln(1/T)$, and p can be found as an angular coefficient of the linear part of the plot $\ln[E_{\text{loc}}/(kT)]$ versus $\ln(1/T)$. As can be seen from figures 3 and 4 (the upper panels), above ~ 310 K (# 3b) and between ~ 290 – 250 K (# 3a) the values of $p = 1.05 \pm 0.05$ and 1.02 ± 0.05 for # 2b and # 2a, respectively, satisfy the NNH conductivity law because equation (2) reduces to equation (1) when $p = 1$. On the other hand, below ~ 280 and 230 K we have the values of $p = 0.75 \pm 0.02$ and 0.77 ± 0.02 for # 2b and # 2a, respectively, coinciding with $p = 3/4$ within the error and differing evidently from $1/2$. In addition, it can be seen that the plots of $\ln \rho$ versus $T^{-3/4}$ (figures 3 and 4, bottom panels) match the linearity at low temperatures better than other plots of $\ln \rho$ versus T^{-p} with $p = 1/4$, $1/3$ or $1/2$ discussed above.

The law $\ln \rho \sim T^{-3/4}$ is the most important disagreement with the 1D models above [13, 14] which deal with the true 1D structures or single isolated 1D chains. Instead, in CaCu_2O_3 we have an array of quasi-1D chains, which fill in the 3D space of the crystal. This is just a case discussed by Fogler, Teber and Shklovskii (FTS) [15]. The main idea of their approach is that they describe such structures as *the 3D array of quasi-1D electron crystals*. The 1D chains are divided by impurities (with the volume concentration N) into segments (rods) with the average length $l = 1/(Na_{\perp}^2)$, where a_{\perp}^2 is the transversal area per chain. The conductivity is metallic inside a rod, whereas hopping charge transfer sets in due to tunnelling of the electrons between different rods along the same chain. At high T

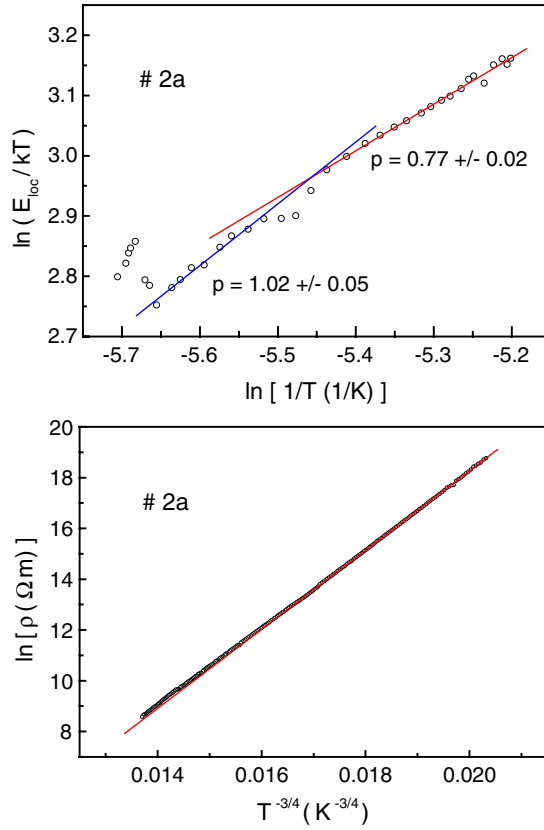


Figure 4. Temperature dependence of the local activation energy (upper panel) and the plot of $\ln \rho$ versus $T^{-3/4}$ for # 2a (lower panel).

they found the conventional NNH conductivity of equation (1) with $E_a \sim e^2/(\kappa l)$ [15]. At low T the Coulomb interactions between the electrons and/or different rods (which may also possess electric charge due to compression by random impurities) in the transversal direction is important. The VRH conductivity law at low T depends on (i) the dimensionality of hopping (tunnelling) $d = 1, 2$ or 3 (ii) the concentration of impurities N and (iii) the character of the Coulomb interactions in the system, which governs the DOS, $g(\varepsilon)$, of charge excitations along the chains, having in the most important cases (neglecting the logarithmical terms) the form $g(\varepsilon) \sim |\varepsilon|^\mu$, where $\mu = 0, 1$ or 2 . The general result of the FTS concept is that the exponent p in equation (2) is given by the expression [15]

$$p = (\mu + 1)/(\mu + d + 1). \quad (4)$$

For convenience we reproduce table 1 from [15] as table 1 of the present paper summarizing all possible values of p in equation (4). As can be seen from table 1 (the value on the intercept of the last column and the last row) for $d = 1$ and $\mu = 2$ we have $p = 3/4$, coinciding with the values of p found above from the analysis of the local activation energy (figures 3 and 4, upper panels). This is a strong argument in favour of the FTS model. Additional evidence can be found below. The law $g(\varepsilon) \sim \varepsilon^2$ means existence of the soft parabolic Coulomb gap Δ near the Fermi energy, like for example in the 3D doped semiconductors [11]. Within the conventional percolation approach [11] we have the maximum hopping energy $E_{\text{max}} = k_B T \xi_c$,

Table 1. The exponent p of VRH conductivity (equation (4)) in the cases of 3D, 2D and 1D tunnelling and a power-law dependent density of states $g(\varepsilon)$ that arises due to 3D Coulomb interactions [15].

| Tunnelling | $g = \text{const}$ | $g \propto \varepsilon $ | $g \propto \varepsilon^2$ |
|------------|--------------------|---------------------------|---------------------------|
| 3D | 1/4 | 2/5 | 1/2 |
| 2D | 1/3 | 1/2 | 3/5 |
| 1D | 1/2 | 2/3 | 3/4 |

where $\xi_c = (T_0/T)^{3/4}$, so that the average hopping energy $E_{\text{av}} \approx E_{\text{max}}/2$. Using the criterion of transition to VRH conductivity over the states of the Coulomb gap in a conventional form $E_{\text{av}} = \Delta$ we find $\Delta \approx (1/2)(T_0^3 T_v)^{1/4}$. From the plots of $\ln \rho$ versus $T^{-3/4}$ (figures 1 and 2) we obtain $\rho_{0v} = 2.42 \times 10^{-6}$ and $1.36 \times 10^{-6} \Omega \text{ m}$, $T_0 = 1.81 \times 10^4$ and $1.73 \times 10^4 \text{ K}$, $T_v \approx 230$ and 300 K for # 2a and # 2b, respectively, yielding $\Delta \approx 0.26$ and 0.27 eV , which means that the Coulomb gap lies entirely inside the electron band $\Delta E \approx E_a = 0.40$ and 0.38 eV for # 2a and # 2b, respectively, and the contradictions like those arising from applications of the 3D and 2D Mott and SE VRH conductivity models (see above) do not exist in the FTS model.

In addition, there are arguments towards the relation of $a_{\perp} \ll l \ll l_s$ (where $2l_s$ is the characteristic length of the distorted region around the impurity centre), which means that the concentration of impurities is high in the investigated material [15]. Indeed, as follows from the FTS model for high N , only the quadratic energy dependence of the DOS exists, whereas for low N we would have a sequence of the laws $g(\varepsilon) \sim |\varepsilon|$ at higher energies and $g(\varepsilon) \sim \varepsilon^2$ at lower energies (cf figure 5 of [15]). This would lead to an interval of the $\ln \rho \sim T^{-2/3}$ dependence followed by the law $\ln \rho \sim T^{-3/4}$ when T is decreased [15]. However, on the plots of $\ln(E_{\text{loc}}/kT)$ versus $\ln(1/T)$ in the upper panels of figures 3 and 4 one can see no intervals of $p = 2/3$, whereas that of $p = 3/4$ is clearly visible and the error in p is sufficiently small to distinguish between the values of $p = 0.67$ and $p = 0.75$.

For high N the characteristic temperature in equation (2) is expressed as

$$T_0 = C_2 \frac{e^2}{\kappa l k_B} \left[\frac{a_{\perp}^2 \sqrt{r_s}}{\xi_{\perp}^2} \ln \left(\frac{l}{a_{\perp}} \right) \right]^{1/3}, \quad (5)$$

where $\xi_{\perp} = a_{\perp} / \ln[e^2 / (\kappa a t_{\perp})]$ is the localization length for interchain hopping, a is the mean distance between the electrons along the chain, t_{\perp} is the interchain hopping integral, $r_s = a/a_B$, $a_B = \hbar^2 \kappa / (m e^2)$ is the Bohr radius (m is the electron effective mass) and C_2 is a constant of the order of unity [15]. Because the values of $E_a \sim e^2 / (\kappa l)$ are very close for both directions, # 2b and # 2a, the values of l should be also close. Hence, from $l = 1 / (N a_{\perp}^2)$ we have close values of a_{\perp} , which is generally in agreement with the CaCu_2O_3 structure. Then we see that the values of ξ_{\perp} can differ only due to t_{\perp} , which differs in # 2b and # 2a by ~ 2.5 times ($t_{\text{leg}} : t_{\text{rung}} : t_{\text{inter}} \approx 5:2:1$, see above) but since ξ_{\perp} depends on t_{\perp} only logarithmically, the values of ξ_{\perp} should be close for # 2b and # 2a, too. Therefore, as far as the average distance between the electrons in both directions could not change significantly, the values of T_0 for # 2a and # 2b should be approximately the same, in agreement with only a $\sim 4\%$ difference between the values of T_0 found from the plots of $\ln \rho$ versus $T^{-3/4}$ above.

Finally, with a logarithmical accuracy (i.e. omitting the logarithmic terms) from equation (5) we have $k_B T_0 \sim e^2 / (\kappa l) r_s^{1/6} \sim E_a r_s^{1/6}$, yielding $r_s \sim (k_B T_0 / E_a)^6 \sim 10^3 \gg 1$; that is, the main condition of applicability of the FTS model, $r_s \gg 1$ [15], is fulfilled well. The localization length along the chain can be expressed as $\xi_x = l/s$, where $s \sim r_s^{1/2} \ln(l/a)$. With the same accuracy we see that $s \sim r_s^{1/2} \gg 1$ and $\xi_x \ll l$, the relations being in line with the FTS model, too [15].

3. Conclusions

We have investigated the resistivity of the spin-ladder compound CaCu₂O₃. The temperature dependence of the resistivity is characterized by an NNH conductivity at high T followed by a VRH conductivity when T is decreased. The analysis of $\rho(T)$ demonstrates that conventional concepts of the hopping charge transfer based on the electron localization in disordered 1D, 2D or 3D systems cannot be applied to interpret our data, leading to intrinsic contradictions including the mismatch of the characteristic energies and/or unphysical values of the characteristic lengths as the localization radius. The most important contradiction is the temperature dependence of the VRH conductivity at low T , which cannot be substantiated within any of the conventional hopping models above. Instead, this dependence finds its clear explanation within a quite different approach proposed recently by Fogler *et al* [15], by treating CaCu₂O₃ as a 3D array of the quasi-1D electron crystals. Additional evidence for applicability of this model is obtained by analysing T_0 and T_v , the characteristic temperature and the onset temperature of the VRH conductivity, respectively, leading to a correct matching of the typical energies as the electron bandwidth and the width of the Coulomb gap in the spectrum of DOS of the charge excitations, and to expectable relations between some typical length scales.

Acknowledgment

One of us (EA) would like to thank DFG for financial support.

References

- [1] Rice T M, Gopalan S and Sigrist M 1993 *Europhys. Lett.* **23** 445
- [2] Dagotto E and Rice T M 1996 *Science* **271** 618
- [3] Dagotto E 1999 *Rep. Prog. Phys.* **62** 1525
- [4] Kiryukhin V, Kim Y J, Thomas K J, Chou F C, Erwin R W, Huang Q, Kastner M A and Birgeneau R J 2001 *Phys. Rev. B* **63** 144418
- [5] Goiran M, Costes M, Broto J-M, Chou F C, Arushanov E, Drechsler S, Buechner B and Kataev V 2006 *New J. Phys.* **8** 74
Sekar C, Ruck K, Krabbes G, Teresiak A and Watanabe T 2002 *Physica C* **378–381** 678
- [6] Lisunov K G, Raquet B, Rakoto H, Broto J M, Xu X Z, Alami H El and Deville Cavellin C 2003 *J. Appl. Phys.* **94** 5912
- [7] Kim T K, Rosner H, Drechsler S-L, Hu Z, Sekar C, Krabbes G, Malek J, Knupfer M, Fink J and Eschrig H 2003 *Phys. Rev. B* **67** 024516
- [8] Plakida N M, Vladimirov A and Drechsler S-L 2004 *Physica C* **408–410** 232
- [9] Vuletic T, Korin-Hamzic B, Tomic S, Gorshunov B, Haas P, Dressel M, Akimitsu J, Sasaki T and Nagata T 2003 *Phys. Rev. B* **67** 184521
- [10] Mott N and Davies E A 1979 *Electron Processes in Non-Crystalline Materials* (Oxford: Clarendon)
Mott N F 1990 *Metal-Insulator Transitions* (London: Taylor and Francis)
- [11] Shklovskii B I and Efros A L 1984 *Electronic Properties of Doped Semiconductors* (Berlin: Springer)
- [12] Borgas E, de Graaf C, Caballol R and Galzardo C 2005 *Phys. Rev. B* **71** 045108
- [13] Yu Z G and Song X 2001 *Phys. Rev. Lett.* **86** 6018
- [14] Serota R A, Kalia R K and Lee P A 1986 *Phys. Rev. B* **33** 8441
- [15] Fogler M M, Teber S and Shklovskii B I 2004 *Phys. Rev. B* **69** 035413